Optical Signature Analysis of Tumbling Rocket Bodies via Laboratory Measurements

H. Cowardin[1], G. Ojakangas[2], M. Mulrooney[3], S. Lederer[4], J.-C. Liou[4]
[1] *ESCG/Jacobs, 2224 Bay Area Blvd., Houston, TX 77058, USA*
[2] *Drury University/LZ Technology*
[3]*ESCG/MEI, 2224 Bay Area Blvd., Houston, TX 77058, USA*
[4]*NASA Orbital Debris Program Office, NASA/JSC, Houston, TX 77058, USA*

ABSTRACT

The NASA Orbital Debris Program Office has acquired telescopic lightcurve data on massive intact objects, specifically spent rocket bodies (R/Bs), to ascertain tumble rates in support of the Active Debris Removal (ADR) studies to help remediate the LEO environment. Tumble rates are needed to plan and develop proximity and docking operations for potential future ADR operations.

To better characterize and model optical data acquired from ground-based telescopes, the Optical Measurements Center (OMC) at NASA/JSC emulates illumination conditions in space using equipment and techniques that parallel telescopic observations and source-target-sensor orientations. The OMC employs a 75-W Xenon arc lamp as a solar simulator, an SBIG CCD camera with standard Johnson/Bessel filters, and a robotic arm to simulate an object's position and rotation. The OMC does not attempt to replicate the rotation rates, but focuses on ascertaining how an object is rotating, as seen from multiple phase angles. The two targets studied are scaled (1:48) SL-8 Cosmos 3M second stages. The first target is painted in the standard Russian government "gray" scheme and the second target is white/orange as used for commercial missions.

This paper summarizes results of the two scaled rocket bodies, each observed in three independent rotation states: (a) spin-stabilized rotation (about the long axis), (b) end-over-end rotation, and (c) a 10° wobble about the center of mass. The first two cases represent simple spin about either primary axis. The third – what we call "wobble" – represents maximum principal axis rotation, with an inertia tensor that is offset from the symmetry axes. By comparing the resultant phase and orientation-dependent laboratory signatures with actual lightcurves derived from telescopic observations of orbiting R/Bs, we intend to assess the intrinsic R/B rotation states. In the simplest case, simulated R/B behavior coincides with principal axis spin states, while more complex R/B motions can be constructed by combinations of OMC-derived optical signatures that together form a rudimentary basis set. The signatures will be presented for specific phase angles for each rocket body and shown in conjunction with acquired optical data from multiple telescope sources.

The results of the data show possible correlations between the laboratory data and telescopic data for the rotations states mentioned above (b) and (c), but with limited data the results were not definitive to differentiate between color schemes and rotations. The only rotation that did not correlate with the observed telescopic data was the spin-stabilized rotation.

1. INTRODUCTION

Capitalizing on optical data products to generate a more complete understanding of orbital space objects is a key objective of the NASA Orbital Debris Program Office's optical measurements program and a primary objective for the Optical Measurements Center (OMC). The OMC is used to emulate space-based illumination conditions using equipment and techniques that parallel telescopic observations and source-target-sensor orientations. Time-dependent optical photometric data yield lightcurves in multiple bandpasses. This aids in material identification and assessment of possible periodic orientations of orbital debris. These data can also be used to help identify shapes and optical properties at multiple solar phase angles (SPA).

This paper focuses on 1:48 scale SL-8 rocket bodies to extract lightcurves for the following rotations: (a) end-over-end, (b) 10° wobble, and (c) spin-stabilized. These three states were chosen based upon the most likely rotational

axes of rocket bodies (a and b) [1] and the simplest rotational state of a cylindrical rocket body (c). The output will be used to develop a database of optical signatures for comparison with and interpretation of telescopic data.

2. DATA ACQUISITION

The design of the OMC is analogous to a telescope set-up with a light source, target, and observer. A 75-W, Xenon arc lamp simulates solar illumination from 200 to 2500 nm. The data are acquired through a Santa Barbara Instrument Group (SBIG) CCD camera (1024 x 1536 pixels) with an attached filter wheel that uses the standard astronomical suite of Johnson/Bessell filters: Blue (B), Visible (V), Red (R), and Infrared (I). For this paper, the data were acquired in the V filter and a clear filter to match telescopic observations of similar targets [2]. The laboratory equipment is capable of obtaining data for a full 360° range in phase angle (the vertex angle between light source, object, and detector) with an accuracy of 1° using a custom-built rotary arm with attached commercial off-the-shelf potentiometer. To prevent scattered light from biasing the observations, a light trap (not shown) is placed directly across from the light source on the other end of the rotary arm, therefore, the data is limited to phase angles between ±(3°- 160°). The layout is shown in Fig.1 with small digital images of the equipment.

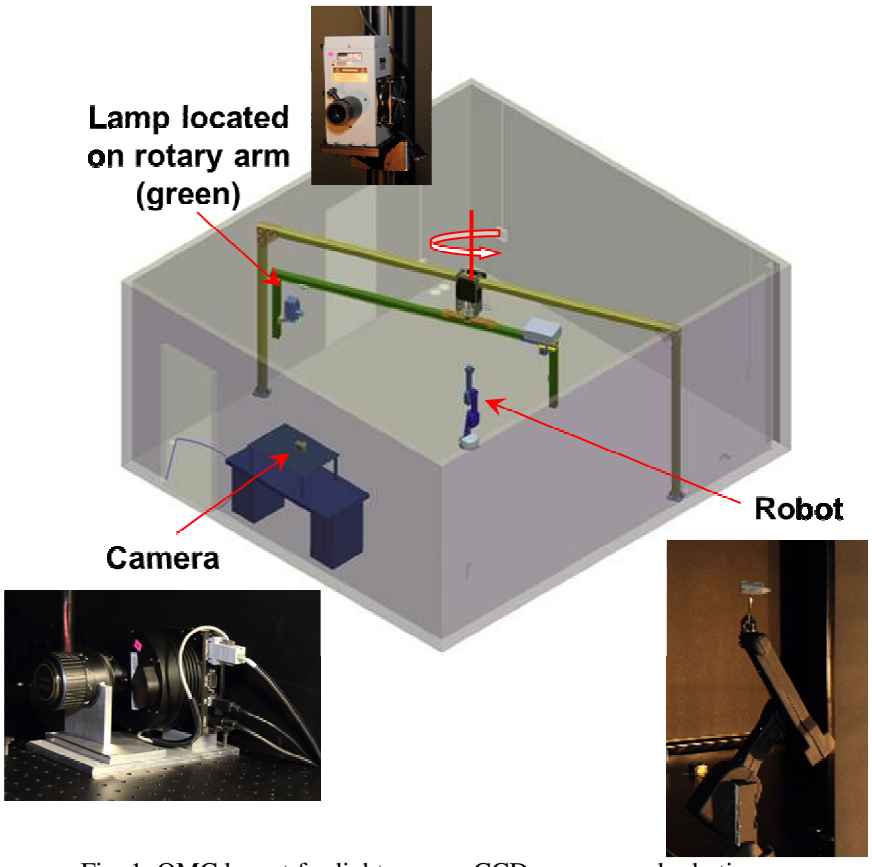

Fig. 1. OMC layout for light source, CCD camera, and robotic arm.

3. TARGET

The NASA Orbital Debris Program Office has acquired telescopic lightcurve data on massive intact objects, specifically spent rocket bodies to ascertain tumble rates in support of the Active Debris Removal (ADR) studies. With a growing population of debris, ADR may play a role in helping to remediate the LEO environment. Tumble rates are needed to plan and develop proximity and docking operations for potential future ADR missions. Using the acquired telescopic data, initial periodic signals were identified, but determining how these periodicities relate to rotation/tumble states requires laboratory and mathematical modeling [1]. Fig. 2 (left) shows the second stage design for SL-8s and a photograph of the two COSMOS-3M launch vehicles (middle). The gray SL-8 (circled in yellow) is primarily used for Russian government missions, while the white with orange paint scheme is dedicated to

commercial missions (also circled in yellow). Simulating telescopic observations of SL-8 rocket bodies was achieved by constructing two 1:48 scale models and painting them to best match actual targets, also shown in Fig. 2 (right). The photographs of the scaled rocket bodies are shown from two different perspectives (note that the white reflective dots on the gray rocket body were used for acquiring 3D scans of these targets and were removed before CCD imaging was conducted).

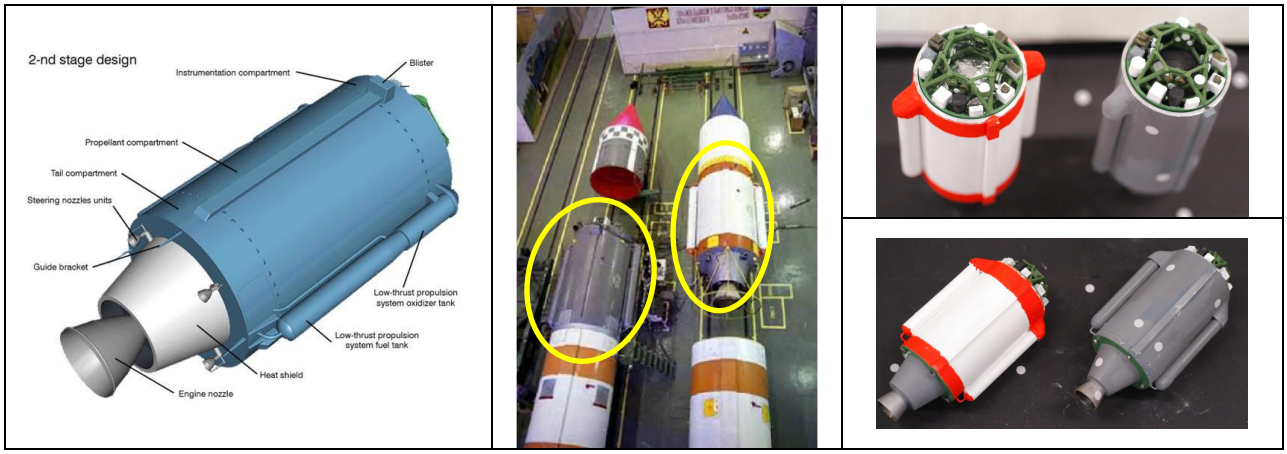

Fig. 2. Left: SL-8 design, courtesy of http://danielmarin.blogspot.com/2010/04/lanzamiento-kosmos-3m-parus-99.html. Middle: Image of two paint schemes used for COSMOS-3M launches, focused on the second stage (circled in yellow), image taken from http://www.b14643.de/Spacerockets_1/East_Europe_3/Kosmos_3/Description/Frame.htm. Right: Scaled SL-8 rocket bodies. Orange/white color scheme is used to model commercial missions, while gray paint scheme best reflects Russian government missions. The top image shows both models as seen from the payload end (using a generic payload struture). The bottom image shows the side view, with thrust (primary rocket nozzle) pointing toward the lower-left.

4. DATA

Three states were used to model the most probable rotational motion for SL-8s: end-over-end, 10° wobble, and spin-stabilized. Although the first two rotational orientations are theoretically more probable [1], the spin-stabilized measurements were made to demonstrate the dramatically different expectations and outcomes in such a case. The laboratory data shown below were largely taken with the clear filter because the majority of the telescopic data were acquired by the New Mexico Skies Observatory (NMSkies), which does not use a filter. The laboratory data taken in Johnson V was used to simulate telescopic data acquired from US Air Force Academy (USAFA).

All data taken in the OMC started with the modeled rocket body mounted with the maximum surface area toward the camera (i.e., side of rocket body). The object was rotated 360° using a robotic arm wrist rotation where the rotational axis is perpendicular to the detector. For small phase angles, the thrust end was imaged at 90° rotation (robot position), then the opposite side of the rocket body at 180°, followed by 270° where the payload end was normal to the camera and lastly back to the original rotation at 360°. Fig. 3 shows the target's rotation from 0°-360° as imaged with the CCD, before post-processing (masking and background subtraction) was completed. The image is depicted in false color to best illustrate the areas where the object is brightest (yellow, orange, and red) and where the image has the lowest reflectivity (blues as shown for the majority of the background). Photographs of the matching orientations are shown at right: side (top image), thrust end (middle), and payload end (bottom).

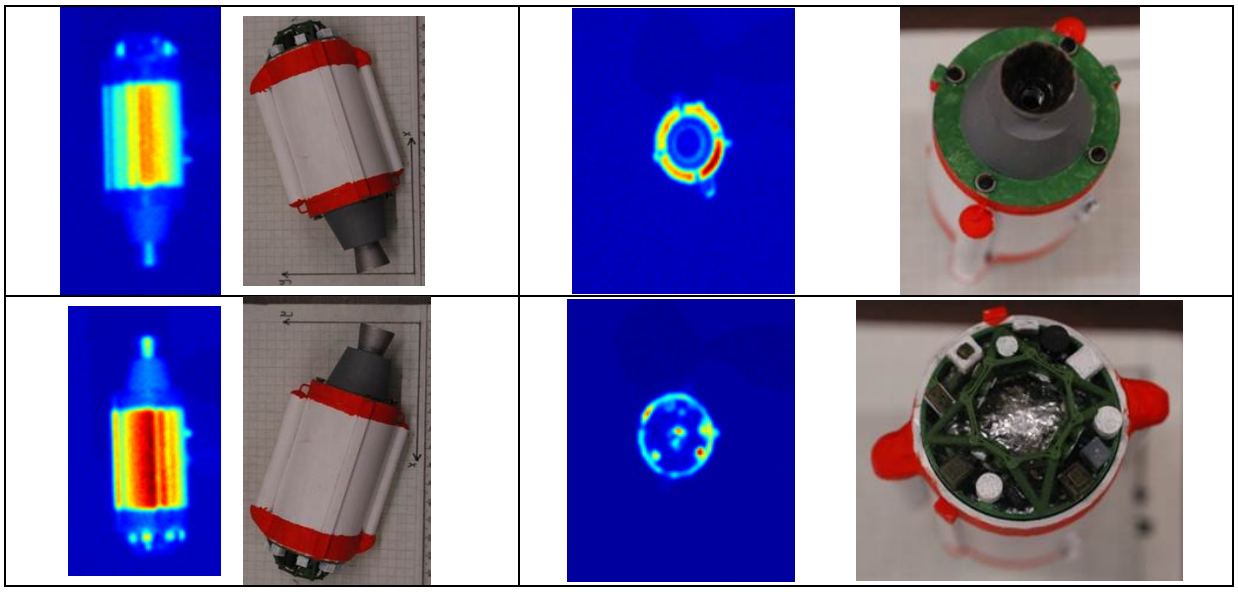

Fig. 3. Left quad-plot: Raw imagery data taken with SBIG CCD using a clear filter showing the OMC rotation sequence for end-over-end orientation (no background subtraction has been applied). Photographs are aligned with rotations representing the side view,thrust end, opposite side view and payload end.

5. RESULTS

The following plots illustrate the two rotations used in the laboratory and how they compare with telescopic observations at roughly the same phase angle. The first data set illustrates multiple lightcurves for the same phase angles observed with NMSkies, starting with the gray rocket body rotated end-over-end (about the shortest axis; mounting method can also be seen in Fig. 8). The images in Fig. 4 show the gray rocket body relative magnitude plots for six different SPAs: 3°, 30°, 60°, 90°, 120° and 150°. The rotation mimics the orientations seen in Fig. 3; therefore, the first, third and fifth peaks (although the first and fifth partial peaks are continuations of each other) at 0°, 180° and 360° rotation angle reflect the brightness when the side panels are normal to the observer. At 90° rotation, the rocket body is orientated such that the thrust is normal to the observer. The payload end is normal to the observer at 270°, which is reflected in the fourth peak (which is the dominant specular peak for small phase angles). This result is not surprising since the rocket body model (payload end) consists of a thin layer of aluminum foil, which is somewhat crinkled and tends to provide multiple facets that additively yield a highly specular response. The discontinuities seen at SPA 130° and 150° are due to low signal returns at those specific rotations. These are defined as “NaN” when the background subtraction process is applied.

The telescopic data shown in Fig. 5 and Fig. 7 have not been range corrected/normalized. Despite this, a useful comparison is still possible between laboratory data and the overall structure of the R/B lightcurves. The lightcurves shown in Fig. 5 represent an SL-8 R/B (Space Surveillance Network (SSN) #: 21231) taken at three different times with increasing phase angle (mean phase angles respectively of <33.6°>, <96.5°>, and <114.8°>). The overall structure of these lightcurves is similar to that of the gray rocket body in Fig 4. For example, the sharp and minor maxima seen in the laboratory dataset match the <96.5°> telecopic observations. It is possible that the two smaller maxima shown in this plot represent the observed intensity when the rocket body’s payload end (near time ~03:08) and thrust end (near time ~03:09) were normal to the observer.

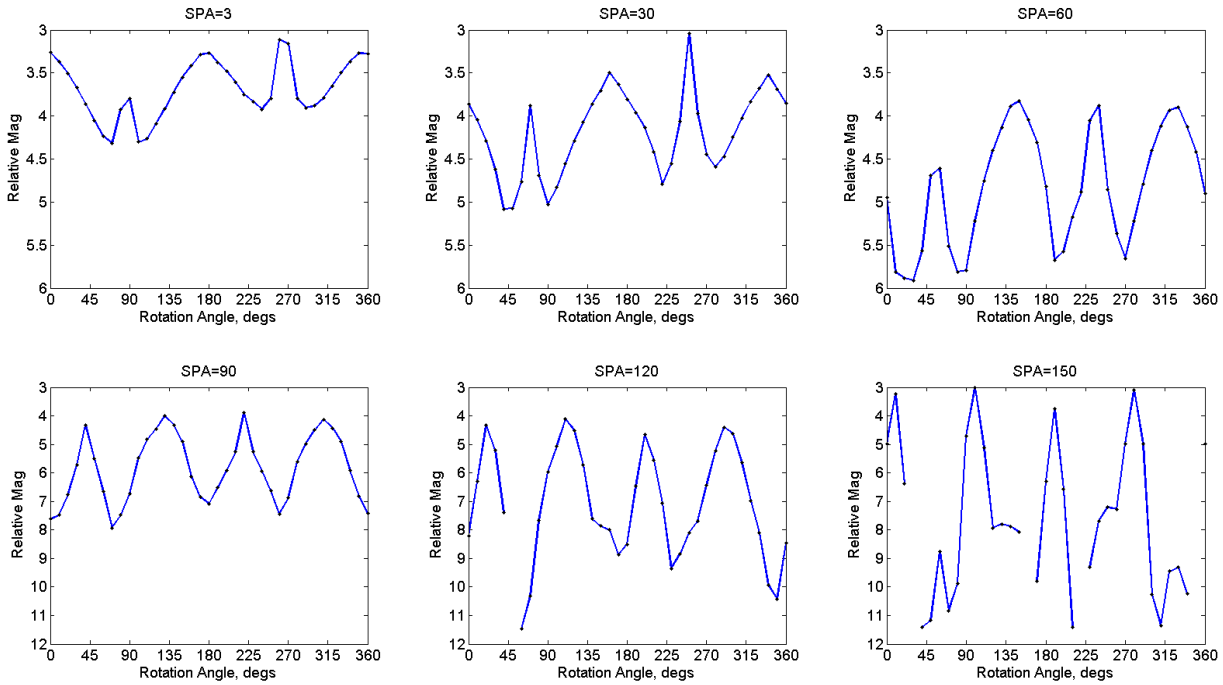

Fig. 4. Relative magnitude lightcurves for gray rocket body rotated end-over-end using a clear filter. Starting from top-left: SPA=3°, 30°, 60°, 90°, 120° and 150°.

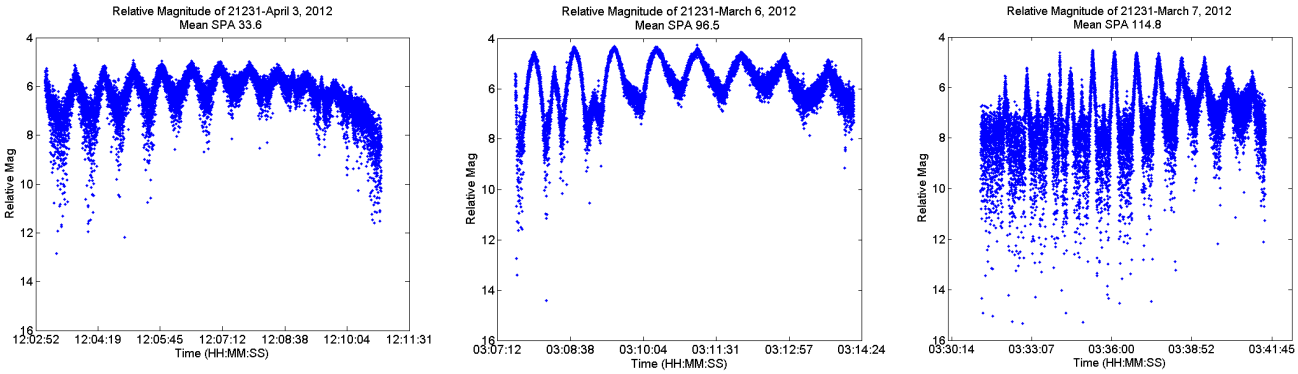

Fig. 5. (Left) Lightcurve plot for SSN 21231 on April 3rd, 2012. <SPA>=33.6°, SPA range 65.9°- 12.0°. (Middle) Lightcurve for SSN 21231 on March 6th, 2012. <SPA>=96.5°, SPA range 93.6°-98.6°. (Right) Lightcurve for SSN 21231 on March 7th, 2012. <SPA> =114.8°, SPA range = 107.8°-118.5°.

Measurements of the second target (white and orange rocket body) used the same mount and rotation configuration as the gray model. The purpose of this experiment was to investigate how different paint schemes can affect the character of the lightcurves (e.g., how the optical signatures vary as a function of [paint] albedo). Similar to the gray model rocket body, four maxima are visible representing the side, payload, and thrust orientations shown in Fig. 6. Unlike the previous model, the maxima representing the sides (~0°, 180° and 360°) exhibit a smoother structure rather than the sharp peak characteristic of the previous laboratory and telescopic data. The exception to this is shown at SPA 150°, where a sharp peak/trough is evident at all four maxima/minima.

The data were compared to another set of telescopic data shown in Fig. 7, SL-8 R/B (SSN #: 29659) with a mean phase angle of <114.7°>. The structure appears to show maxima that are smoothly varying with one minor sharp peak seen near 180 seconds. The observed mean SPA for the telescopic data was 114°, which best matches the 120° laboratory plot in Fig. 7 (bottom-middle). Further investigation into the possibility of correlating the laboratory produced lightcurves with telescopic data based on varying paint schemes proved to be indeterminate, as SSN 29659 employs the gray paint scheme.

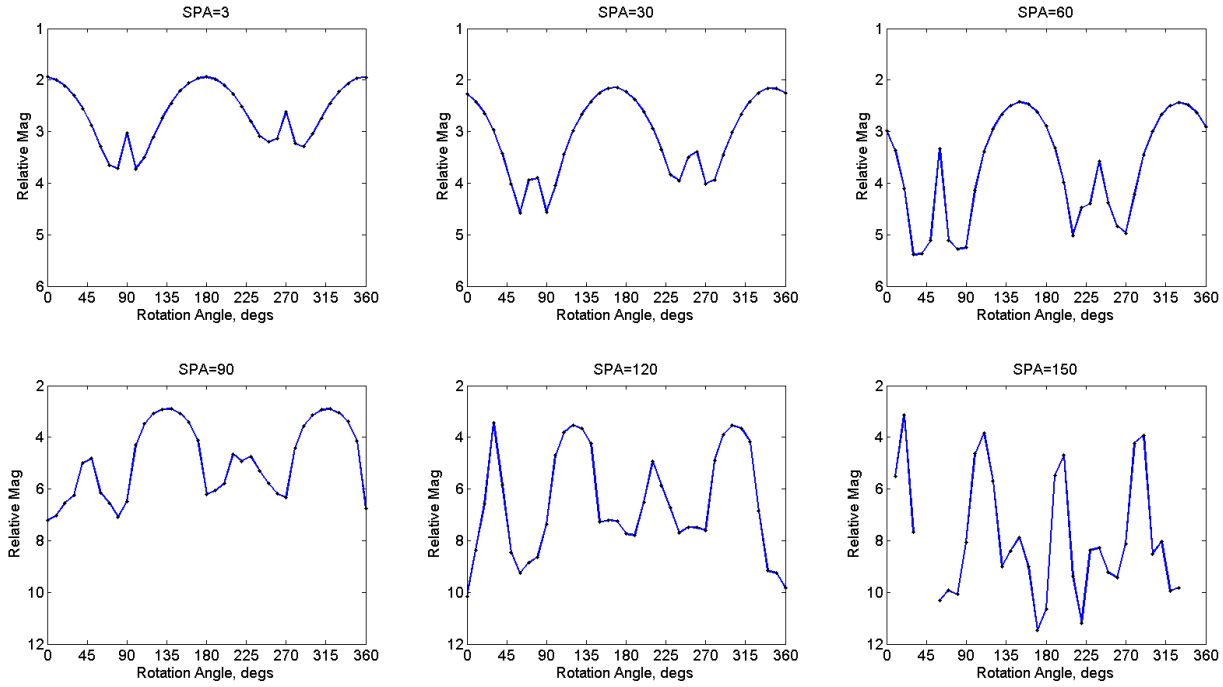

Fig. 6. Relative magnitude lightcurves for white and orange rocket body rotated end-over-end using a clear filter. Starting from top-left: SPA=3°, 30°, 60°, 90°, 120° and 150°.

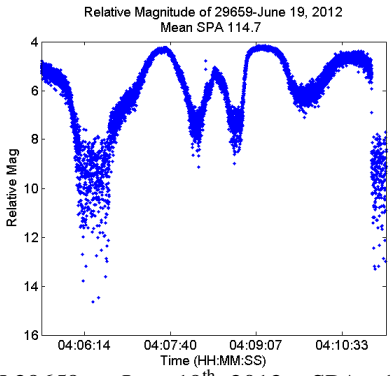

Fig. 7. Lightcurve plot for SSN 29659 on June 19th, 2012. <SPA> 114.7°, SPA range 82.8°-138.8°

Before any conclusions can be drawn about the correlation between telescopic data and laboratory data, an additional rotation sequence will be shown – that of a wobbling R/B. To generate this sequence the rotation axis was tapped at 10° to the R/B normal (defined as the R/B short axis). The hole was set adjacent to the end-over-end mount hole so the axis of rotation passed through the model's center of mass (as estimated by literature research on a SL-8 dry mass). Fig. 8 shows a diagram of the two mounting holes, where the red arrow indicates the axis for end-over-end rotation and the blue arrow points to the axis of rotation for the 10° wobble.

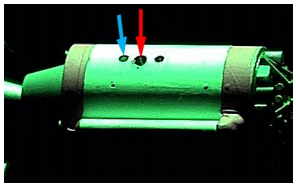

Fig. 8. Mount holes on rocket body for robotic arm. Blue arrow points to 10 degree wobble mount and red arrow points to end-over-end rotation mount, which passes through the center of mass.
The non-specified hole to the right of the red arrow is for future measurements.

The plots shown in Fig. 9 illustrate the lightcurves for the gray rocket body undergoing a 10° wobble for multiple phase angles: 3°, 30°, 60°, 90°, 120° and 150°. One noticeable difference between the rotations is that the minor peaks associated with the payload and thrust ends are not as prominent at lower phase angles (3° and 30°). The amplitude for the two minor peaks at 3° SPA is on the order of 0.3 magnitudes for the 10° wobble versus ~1 magnitude for the end-over-end rotation (as shown in Fig. 10). The overall structure remains the same though, making it difficult to distinguish in a blind study whether the lightcurves are those of an end-over-end rotation or 10° wobble. For the gray R/B at SPA =150° both rotation states (wobble and end-over-end) display lightcurves with more features. This may be attributed to specular reflections from the target when the majority of the reflections were forward scattering.

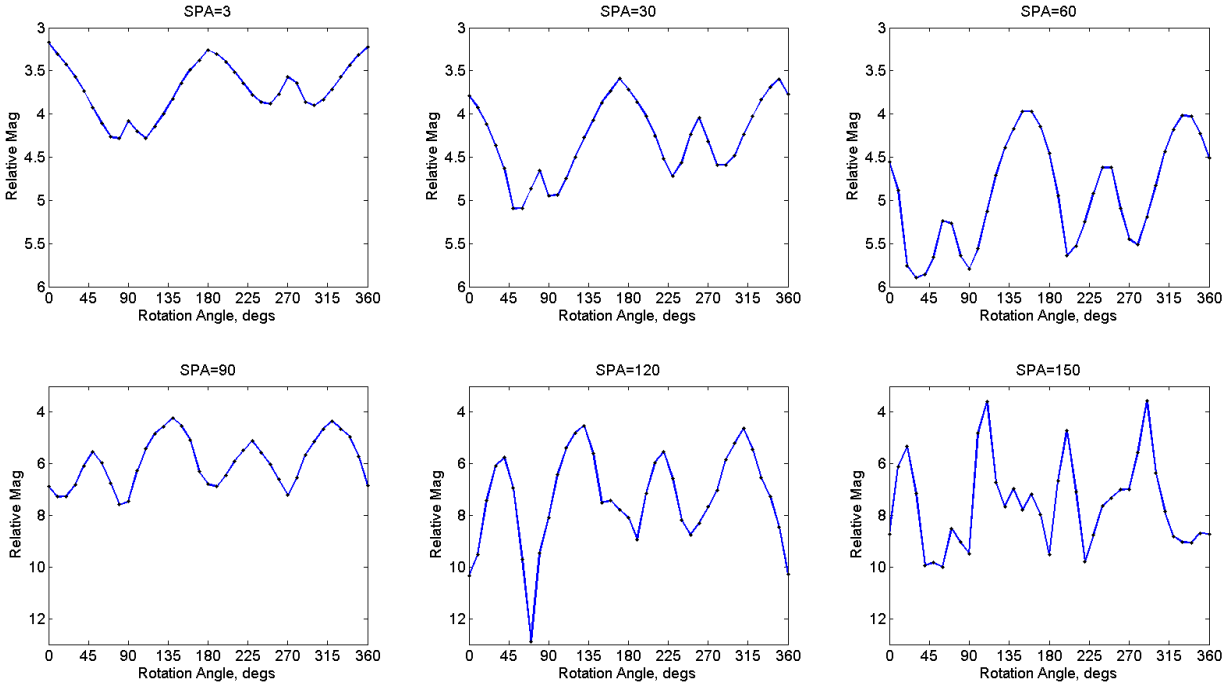

Fig. 9. Relative magnitude lightcurves for gray rocket body rotated with 10° wobble using a clear filter. Starting from top-left: SPA=3°, 30°, 60°, 90°, 120° and 150°.

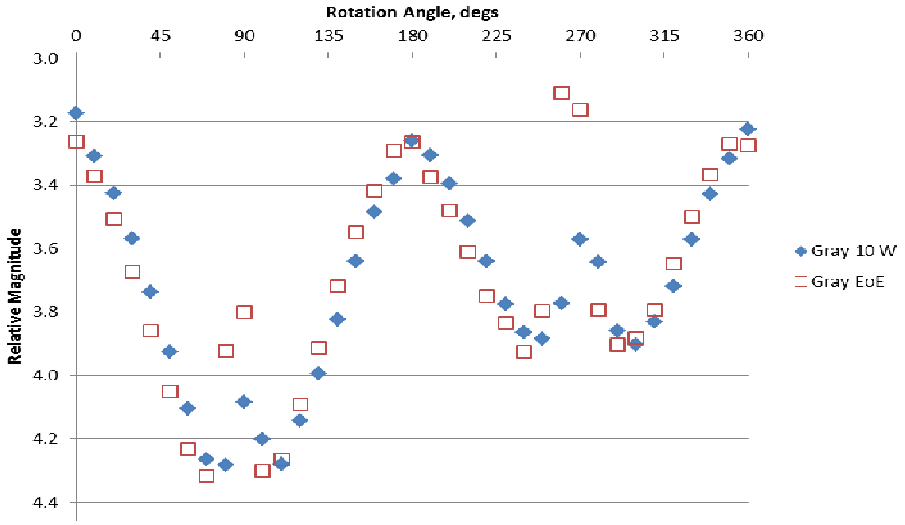

Fig. 10. Relative magnitude comparison at 3° SPA using gray rocket body for 10° wobble (Gray 10 W) and end-over-end rotation (Gray EoE).

Fig. 11 illustrates relative magnitude vs. rotation angle for the white and orange rocket body under the same rotation as the gray target for the same set of phase angles. Like the gray rocket body, the overall characteristics of the white and orange rocket body in a 10° wobble look similar to that of an end-over-end rotation; the only distinguishable difference is the weakness of the relative amplitudes of the minor peaks caused by the thrust and payload. The difference between the two minor peaks at 3° SPA is shown in Fig. 12 for the white and orange rocket body during a 10° W and end-over end rotation state. The difference between the two peaks for each state is <0.3 magnitudes for the 10° wobble versus ~0.6 magnitudes for the end-over-end case.

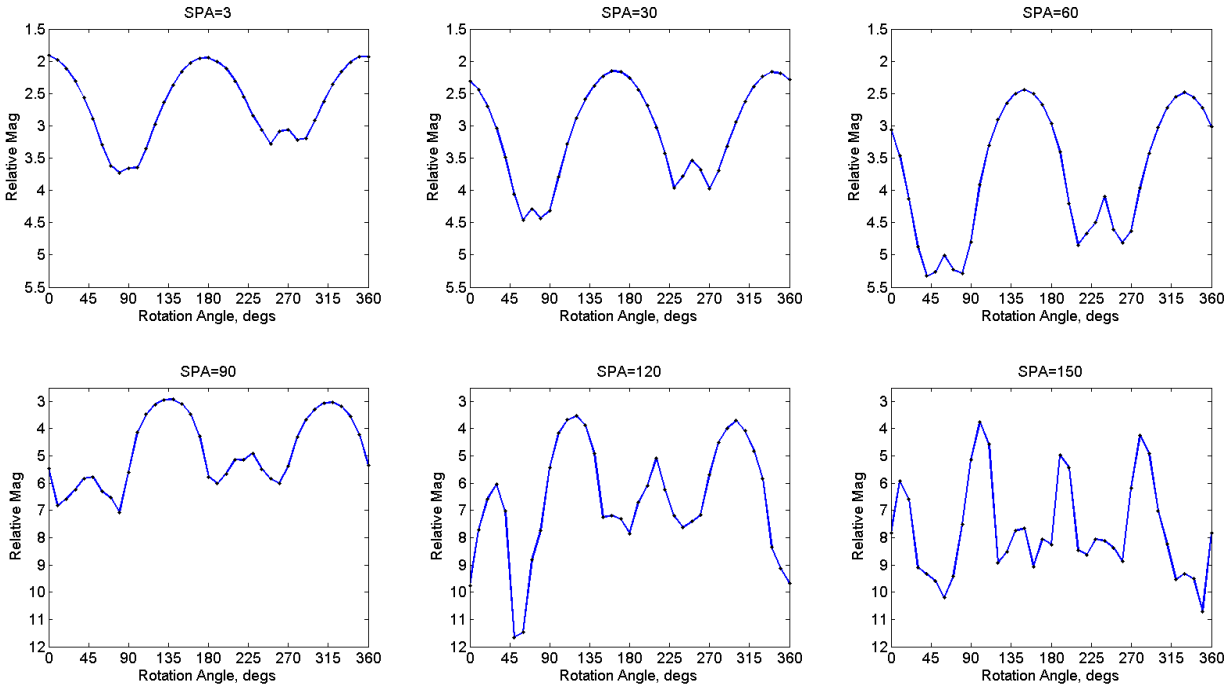

Fig. 11. Relative magnitude lightcurves for white and orange rocket body rotated with 10° wobble using a clear filter. Starting from top-left: SPA=3°, 30°, 60°, 90°, 120° and 150°.

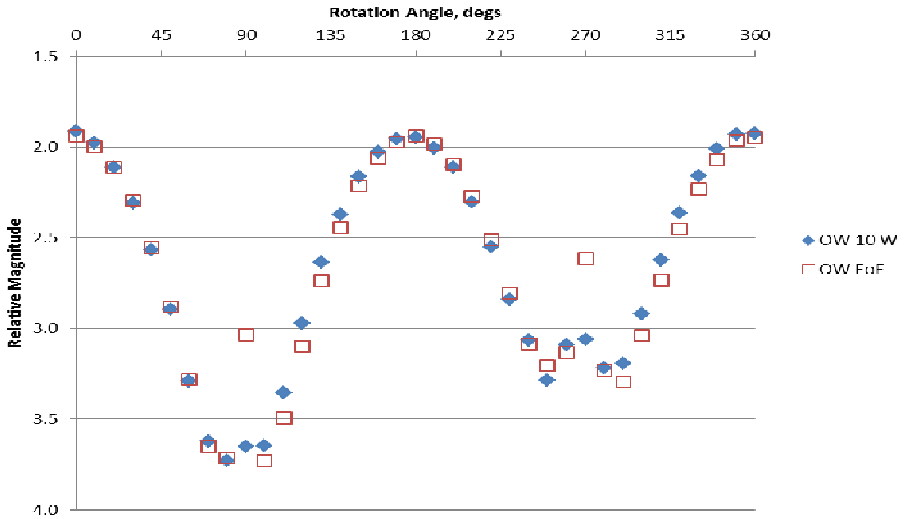

Fig. 12. Relative magnitude comparison at 3° SPA using orange and white rocket body for 10° wobble (OW 10 W) and end-over-end rotation (OW EoE).

To better assess the differences in the optical signatures between the two paint schemes, a laboratory exercise was performed using simple cylinders painted flat (matte) black and shiny (glossy) black. Fig. 13 shows the results of the

diffuse versus specular study using a black cylinder. The painted black cylinders show optical characteristics similar to both SL-8 rocket bodies (two maxima, two minima), but the flat black cylinder mimics the smooth characteristics seen in the white/orange rocket body, whereas the shiny black cylinder exhibits sharper peaks when the side of the cylinder (0°, 180°, 360° for 3° SPA) is normal to the observer, as seen with the gray rocket body. The white/orange model was coated with a clear flat finish, providing a diffuse reflection, whereas the gray rocket body model had a sheen reflection on the target, providing a more specular response (possibly due to oxidation or handling). Research into actual photographs of SL-8 rocket bodies shows the paint has more of a "satin" finish, which will be applied to future models. The laboratory data will be compared to modeled lightcurves of SL-8 targets [1] in order to better estimate the specular/diffuse ratio of observed targets.

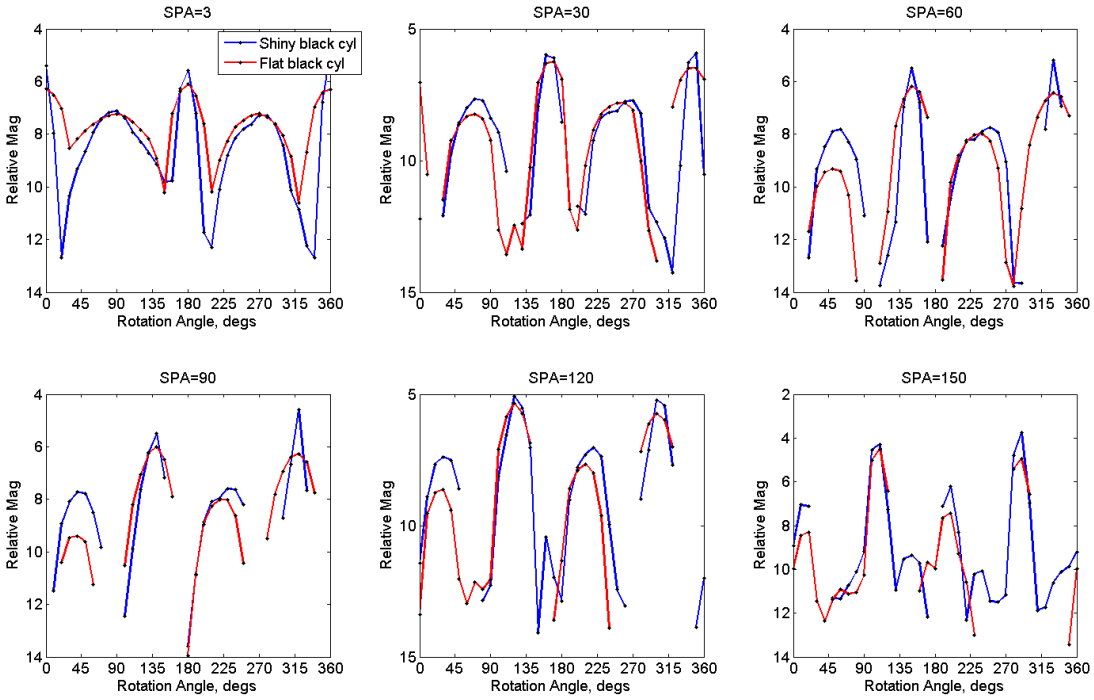

Fig. 13. Relative magnitude for shiny black simple cylinder and flat, matte black cylinder in an end-over-end rotation.

The last set of lightcurves simulates a rocket body in a spin-stabilized state. Here, the scaled images of the rocket body are shown for specific rotation angles; from top left-right: 0°, 90°, 180°, and 270° rotation (shown in Fig. 13). As mentioned previously, this rotation is theorized to be one of the least likely possibilities for these specific spent rocket bodies based on their non-spin-stabilized states at time of orbit injection. Furthermore, if such R/Bs were spin stabilized, the rotational state would probably evolve, in a timescale of weeks, toward maximum-axis rotation due to internal friction and magnetic induction torques [1]. The lightcurves shown in Fig. 14 illustrate what one could expect for similar targets (R/Bs) in a spin-stabilized state. Unlike a simple cylindrical target rotating about its longest symmetrical axis, the SL-8 R/B has two side-mounted fuel tanks that contribute significantly to the optical signature seen in the laboratory data. Specifically, in Fig 14 when the rocket body is oriented such that the fuel tanks are normal to the observer (between 50°-150° and 300°-325° rotation for 3° SPA) the relative intensity decreases, which corresponds to the minima.

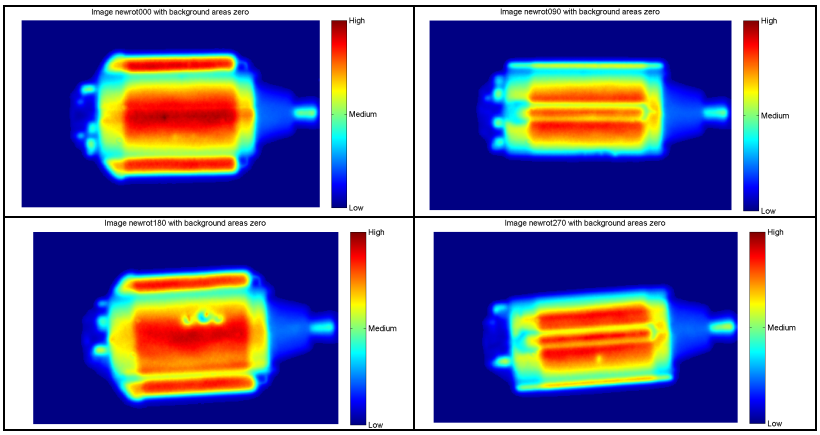

Fig. 13. Four images showing different orientations of the orange and white model rocket body in a spin-stabilized rotation, from top left-right: 0°, 90°, 180°, and 270° rotation. The images are scaled so the dark blue represents low intensities (near 0) and the red colors show the brightest intensities. These images are taken after the background has been subtracted, which is why the majority of the background is dark blue.

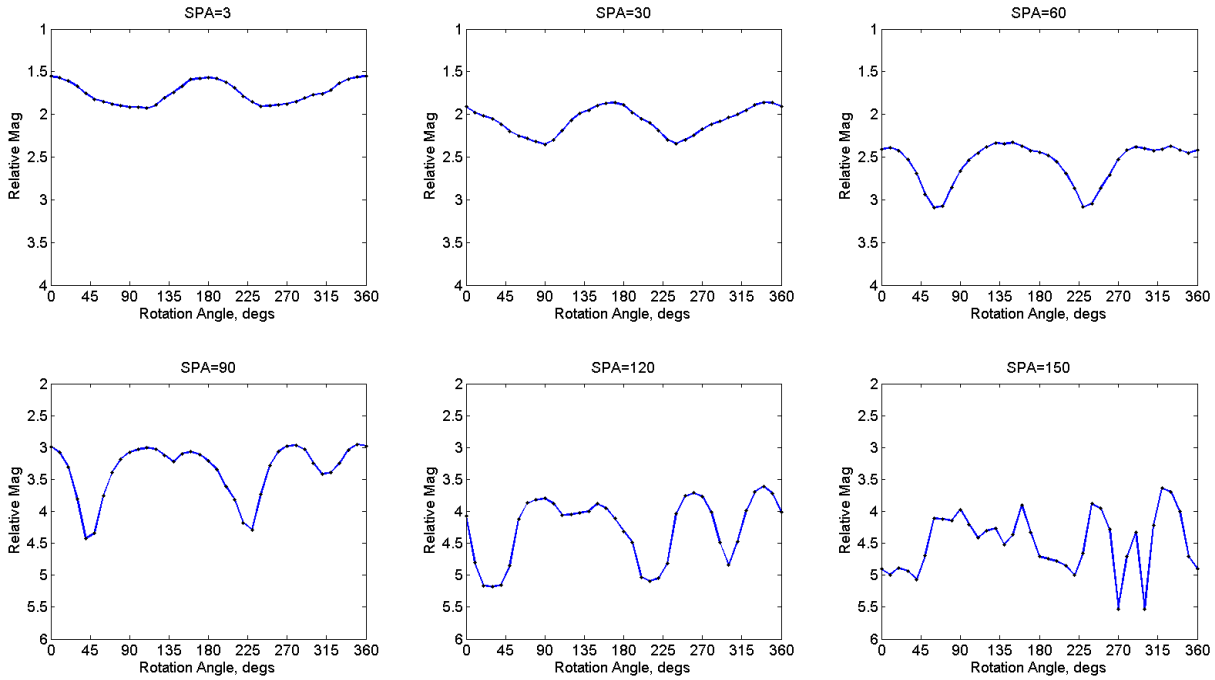

Fig. 14. Relative magnitude lightcurves for white and orange rocket body in a spin-stabilized rotation using a clear filter.

6. Conclusions

The purpose of this paper is not to provide the definitive conclusions as to how R/B targets are rotating, but rather to offer insight into the lightcurves one might expect based on the behavior of scaled, realistic SL-8 targets for three possible rotations states: two theoretically probable states (wobble and end-over-end) and one commonly assumed, but theoretically and operationally unlikely state (long axis spin-stabilized). We do conclude, however, that lightcurves generated from telescopic observations of R/Bs are highly dependent on target orientation as defined by their rotation states (i.e., time-dependent aspect angle). This contention is supported by the fact that many R/B lightcurves show optical signatures whose behaviors are independent of phase angle. Our laboratory data also bear this out by demonstrating that lightcurves depend significantly upon rotation states and less so on phase angle.

The majority of the telescopic lightcurves did show sharp peaks in the maxima/minima similar to the laboratory lightcurves for the gray R/B. Although the lightcurve structure of the white/orange R/B model matched that of an observed SL-8, the paint scheme of the observed target was determined to be gray. A simple study of diffuse versus specular coatings on a simple cylinder proved specular (glossy) coatings do show sharp peaks in the maxima while diffuse (matte) coatings are smoother. After further investigation into the model rocket bodies, the primary white rocket body coating was found to be mostly diffuse while the gray rocket body model showed a more specular coating. To better correlate optical signatures constructed in the laboratory with telescopic data, the authors will investigate the various specular/diffuse ratios of SL-8 rocket body models using lightcurve model code developed by G. Ojakangas [1].

While there was a small morphological difference between the end-over-end rotation and 10° wobble, this was only seen in the laboratory data for the minor secondary peaks that reflect light when the payload or thrust ends are normal to the observer. There is not enough difference between these two orientations to definitively correlate telescopic data with laboratory data. Incidentally, the majority of the telescopic data deemed as "periodic" were best matched by the laboratory data for the gray rocket body.

To further investigate how albedo contributes to optical signature characteristics, a third rocket body will be built to match the white and orange rocket body dimensions, but with a darkened/browned paint in place of the white paint to simulate space weathering affects. This will also help with investigations into diffuse and specular effects relative to acquired optical signatures.

Additional laboratory data will also be acquired to investigate rotations that are more complicated and other rocket body models (e.g., SL-16s) in hopes of providing better insight into how spent rocket bodies are tumbling in space.

7. REFERENCES

1. Ojakangas, G., et al., Probable Rotation States of Rocket Bodies in Low Earth Orbit, 2012 AMOS Technical Conference Proceedings, Kihei, Maui, HI, 2012.

8. ACKNOWLEDGEMENTS

The authors would like to acknowledge the following individuals who provided telescopic data for use in this paper: J. Read (ESCG\HS) and F. Chun, M. Dearborn, and R. Tippets (all from the Department of Physics, U.S. Air Force Academy). The USAFA observations were funded by the NASA/JSC Center Innovation Research and Development Program. Also, thanks to John Lambert for his technical insight related to rotating rocket bodies. We would also like to thank Todd Dicken (University of West Virginia), Spenser Kockler (Drake University), and Virginia Price (Montana State University) for their contributions with OMC calibrations and initial data acquisition. Lastly, thanks to Phillip Anz-Meador and ESCG/Jacobs Technology for providing the scaled rocket bodies for use in the OMC.